Neurochem Res (2013) 38:2385–2396
DOI 10.1007/s11064-013-1151-8

ORIGINAL PAPER

Decreased NAA in Gray Matter is Correlated with Decreased Availability of Acetate in White Matter in Postmortem Multiple Sclerosis Cortex

S. Li · R. Clements · M. Sulak · R. Gregory · E. Freeman · J. McDonough

Received: 13 May 2013 / Revised: 2 August 2013 / Accepted: 5 September 2013 / Published online: 29 September 2013

Abstract Multiple sclerosis (MS) is an inflammatory neurodegenerative disease of the central nervous system (CNS) which leads to progressive neurological disability. Our previous studies have demonstrated mitochondrial involvement in MS cortical pathology and others have documented decreased levels of the neuronal mitochondrial metabolite *N*-acetyl aspartate (NAA) in the MS brain. While NAA is synthesized in neurons, it is broken down in oligodendrocytes into aspartate and acetate. The resulting acetate is incorporated into myelin lipids, linking neuronal mitochondrial function to oligodendrocyte-mediated elaboration of myelin lipids in the CNS. In the present study we show that treating human SH-SY5Y neuroblastoma cells with the electron transport chain inhibitor antimycin A decreased levels of NAA as measured by HPLC. To better understand the significance of the relationship between mitochondrial function and levels of NAA and its breakdown product acetate on MS pathology we then quantitated the levels of NAA and acetate in MS and control postmortem tissue blocks. Regardless of lesion status, we observed that levels of NAA were decreased 25 and 32 % in gray matter from parietal and motor cortex in MS, respectively, compared to controls. Acetate levels in adjacent white matter mirrored these decreases as evidenced by the 36 and 45 % reduction in acetate obtained from parietal and motor cortices. These data suggest a novel mechanism whereby mitochondrial dysfunction and reduced NAA levels in neurons may result in compromised myelination by oligodendrocytes due to decreased availability of acetate necessary for the synthesis of myelin lipids.

Keywords *N*-acetyl aspartate · Acetate · Mitochondria · Multiple sclerosis

S. Li · R. Gregory
Department of Chemistry and Biochemistry, Kent State University, Kent, OH 44242, USA

R. Clements · M. Sulak · E. Freeman · J. McDonough (✉)
Department of Biological Sciences, Kent State University, Kent, OH, USA
e-mail: jmcdonou@kent.edu

Introduction

MS is an inflammatory, demyelinating disease of the CNS that destroys myelin, oligodendrocytes, axons, and neurons [1]. In MS, autoimmune mediated demyelination results in conduction abnormalities and neurological disability. In relapsing remitting forms of disease, conduction is restored after inflammatory episodes due to redistribution of sodium channels and remyelination by oligodendrocytes [2]. Over time, many patients progress to secondary progressive forms of disease. Even though inflammation is decreased in this later stage of disease, chronic damage to axons and neurons results in permanent disability [3]. One of the most critical events leading to damage to axons and neurons and increasing disability over time is the inability to remyelinate exposed axonal segments. Understanding the crosstalk between neurons and oligodendrocytes is critical in order to uncover mechanisms involved in remyelination in the CNS. The neuronal mitochondrial metabolite NAA is a likely candidate for mediating crosstalk between neurons and oligodendrocytes due to the fact that it is synthesized by the enzyme aspartate *N*-acetyltransferase in neuronal mitochondria and is metabolized by aspartoacylase (ASPA) which is found primarily in oligodendrocytes to give rise to acetate and consequently acetyl-CoA [4] as shown in Fig. 1. The significance of this relationship has been

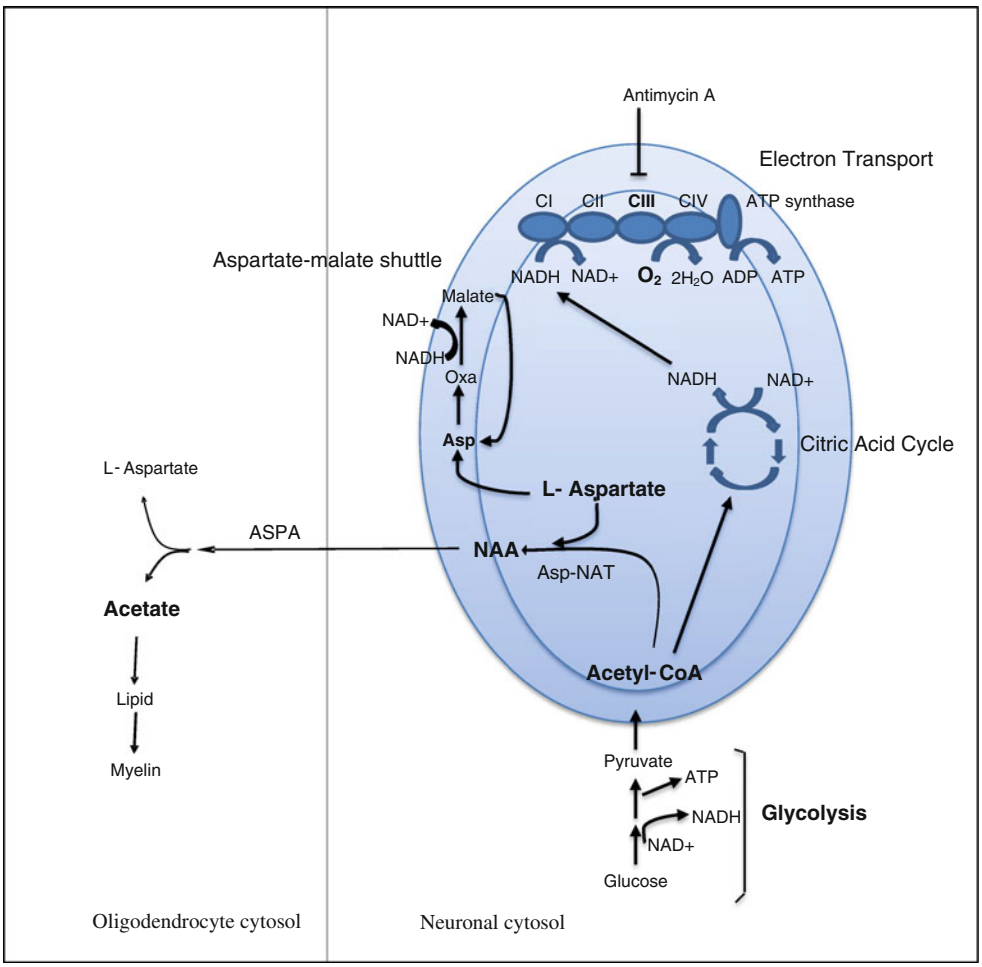

Fig. 1 Schematic depicting NAA metabolic reactions and their relationship to energy metabolism pathways. Diagram depicts the reactions involved in NAA synthesis from L-aspartate and acetyl-CoA in neuronal mitochondria and subsequent catabolism by ASPA to aspartate and acetate in the cytosol of oligodendrocytes. Substrates and pathways measured or perturbed in SH-SY5Y cells (NAA, L-aspartate, acetyl-CoA, complex III, oxygen consumption rate (OCR), glycolysis) or in postmortem brain samples (NAA and acetate) in this study are shown in *bold*. Neuronal mitochondria are represented by the *large blue oval* showing the outer and inner mitochondrial membranes. Energy metabolism pathways relevant to this study including glycolysis, the citric acid cycle, the electron transport chain, and the aspartate-malate shuttle are shown schematically. *NAA N*-acetyl aspartate, *ASPA* aspartoacylase, *Asp-NAT* aspartate-*N*-acetyltransferase, *asp* L-aspartate, *oxa* oxaloacetate, *CI-CIV* complexes I-IV of the electron transport chain (Color figure online)

suggested to involve the use of NAA as an essential substrate for lipid synthesis and myelination in the CNS [5]. This suggestion is supported by the demonstration that NAA contributes acetyl groups for the synthesis of lipids which are in turn incorporated into myelin [6, 7].

NAA has been found to be decreased in the MS brain as measured in postmortem tissue by HPLC or in vivo by magnetic resonance spectroscopy (MRS) [8–12]. These studies have also shown that decreased NAA is correlated with disability and cognitive impairment in MS. NAA has traditionally been considered a marker of neuronal integrity and decreases in NAA in neurodegenerative diseases such as MS have been interpreted as measures of axonal loss and brain atrophy. Measurements of both NAA and brain volume by magnetic resonance imaging (MRI) however, have shown that there are considerable decreases in NAA which precede neuronal atrophy [13]. Indeed other MRS studies have shown that decreases in NAA in MS are reversible in remitting phases of disease indicating that decreased NAA is due to a temporary insult such as a dysfunction in neuronal metabolism rather than a more long term insult such as neurodegeneration [14–16]. Thus, decreased NAA is not merely a marker of neuronal loss but also an indication of dysfunction of neuronal metabolism prior to neuronal degeneration. MS has been traditionally considered a white matter disease but some studies have shown that cortical pathology, including gray matter lesions and cortical atrophy, is extensive [17–19]. Pathological correlates of cortical damage in MS include fatigue and cognitive impairment [20]. The mechanisms involved in cortical

Table 1 Donor Tissue Descriptions

Sample	Sex	Age (years)	PMI (h)	Region	DD (years)	Cause of death	Lesion status
MS tissue							
MS1	M	63	9.0	MC	30	Brain cancer	NAGM/NAWM
MS2	F	67	2.5	MC	–	–	GML/NAWM
MS3	F	69	4.0	MC	–	–	GML/NAWM
MS4	M	59	3.0	MC	–	–	NAGM/NAWM
MS5	F	45	10.0	MC	23	Pneumonia	GML/NAWM
MS6	M	48	3.5	Parietal	–	Myocardial infarction	NAGM/NAWM
MS7	F	53	3.0	Parietal	–	–	NAGM/NAWM
MS8	M	66	3.0	Parietal	46	Pneumonia	NAGM/NAWM
MS9	F	36	3.0	Parietal	14	–	NAGM/NAWM
MS10	F	85	5.0	Parietal	51	Pneumonia	NAGM/NAWM
MS11	F	62	6.0	Parietal	6	Head trauma	NAGM/NAWM
Control tissue							
C1	M	73	4.0	MC		–	
C2	F	63	21.0	MC		–	
C3	M	58	–	MC		–	
C4	F	49	5.0	MC		–	
C5	M	65	6.5	Parietal		Respiratory failure	
C6	F	86	–	Parietal		–	
C7	M	87	3.0	Parietal		Adenocarcinoma	

Motor cortex (MC) was analyzed from five MS (MS1–5) and four control (C1–4) cortical tissue blocks. Parietal cortex was analyzed from six MS (MS6–11) and three control (C5–7) cortical tissue blocks. *PMI* postmortem interval, – not available, *DD* disease duration, *NAGM* normal appearing gray matter, *NAWM* normal appearing white matter, *GML* subpial gray matter lesion

pathology aren't clear, but several studies analyzing postmortem MS tissue have reported mitochondrial damage in MS cortex [21–25]. In these studies expression of the mitochondrial transcription factor PPARGC1 was decreased in neurons and expression of electron transport chain gene mRNA and protein were significantly decreased in normal appearing gray matter (NAGM) in MS cortex compared to controls. Further, these studies identified deletions of mitochondrial DNA and decreased activity of electron transport chain complexes in NAGM in MS. In the present study we have investigated the potential downstream effects of dysfunctional mitochondria on MS cortical pathology. We have examined the relationship between mitochondrial activity and NAA synthesis and have measured the levels of NAA and its breakdown product, acetate, in postmortem MS and control parietal and motor cortex.

Materials and Methods

Postmortem Tissue

Postmortem frozen brain tissue was obtained from the Rocky Mountain MS Center (Englewood, CO). Donor demographics are shown in Table 1. Tissue was matched for brain region, age, and postmortem interval as closely as possible. MS and control postmortem cortex was analyzed for the metabolites NAA and acetate. Frozen blocks of brain tissue were sectioned into 60 μm slices on a cryostat. Gray and white matter were separated with a razorblade at the time of sectioning, and stored in separate 50 mL Falcon tubes at −80 °C. 50–100 mg tissue was collected for analysis. During tissue collection, selected sections from each sample were affixed to microscope slides rather than being placed into a Falcon tube. Immunohistochemistry with an anti-myelin proteolipid protein (PLP) antibody was performed on these sections to determine lesion status. Frozen sections were fixed in 70 % ethanol and treated with 1 % hydrogen peroxide to quench endogenous peroxidase activity. They were subsequently blocked in 3 % donkey serum and incubated with a monoclonal antibody to PLP (Millipore, Temecula, CA) diluted 1:200 in PBS containing 3 % donkey serum and 0.5 % Triton-X overnight at 4 °C. They were then incubated with biotinylated donkey anti-mouse secondary diluted 1:500 overnight at 4 °C followed by incubation in Vector Elite ABC horseradish peroxidase solution (Vector Laboratories, Burlingame, CA). PLP was visualized as a brown precipitate developed with the diaminobenzidine (DAB) reaction.

Cell Culture

SH-SY5Y cells were cultured in 1:1 mixture of EMEM and F-12 medium (Sigma-Aldrich, St. Louis, MO) with 10 % FBS (MidSci, St. Louis, MO) until 90 % confluent. The cells were treated with 2.5 μM antimycin A (Sigma-Aldrich, St. Louis, MO) for 1 and 4 h prior to NAA measurements. This concentration of antimycin A has been previously shown to inhibit respiration in SH-SY5Y cells [26]. Cell viability was monitored by trypan blue assay. Briefly, 4×10^6 SH-SY5Y cells were seeded into 12 well plates until 90 % confluent. The cells were treated with 2.5 μM antimycin A for 1 or 4 h. The cells were detached, centrifuged at 2,000*g* for 4 min and resuspended in 500 ml fresh medium. The cell suspension was mixed 1:1 with trypan blue solution and incubated for 5 min. Cell numbers were counted under microscope using a hemocytometer. To quantify neurites, SH-SY5Y cells were differentiated with retinoic acid and then treated with 2.5 μM antimycin A for 4 h, fixed, and stained with an antibody to neurofilament (Chemicon, Temecula, CA) and Topro to stain nuclei. Images were acquired with an Olympus FV500 confocal microscope and neurites were counted for 24 cells on each cover slip.

NAA Quantitation by HPLC

The neuronal mitochondrial metabolite NAA was quantitated in postmortem brain tissue and in cultured human SH-SY5Yneuroblastoma cells by HPLC. For brain tissue, NAA was quantitated from gray matter from the same tissue blocks analyzed for acetate concentration from both control and MS patients. For SH-SY5Y cells NAA levels were quantified before and after treatment with the mitochondrial electron transport chain inhibitor antimycin A. For HPLC, 50–100 mg postmortem brain tissue or 4×10^6 SH-SY5Y cells were homogenized in ice-cold 90 % methanol using pellet pestle, and centrifuged twice at 14,000 rpm for 10 min at 4°C. The supernatant was dried by speed-vac. The powder was then dissolved in 0.5 ml deionized H_2O and the solution was added to an AG50W × 8 poly-pre columns (Bio-Rad, Hercules, CA). The column was washed with 1 ml of deionized H_2O, and all the eluate was collected, lyophilized, and stored at 4 °C. For HPLC analysis, each sample was resuspended in 300 μl deionized H_2O. A Whatman partisil 10 SAX anion-exchange column (4.6 mm × 250 mm) was used in an Agilent 1100 Series HPLC Value System (Agilent Technologies, Santa Clara, CA). The mobile phase consisting of 0.1 M KH_2PO_4 and 0.025 M KCl at pH 4.5 was prepared before use. After washing the column with 50 % acetonitrile and 50 % deionized H_2O, the column was conditioned with at least 20–30 column volumes of new mobile phase. Retention data were collected at a flow-rate of 1.5 ml/min. The flow was monitored with an Agilent 1100 series UV detector at 214 nm. Retention time was 5.10 min and was determined with an NAA standard (Sigma-Aldrich, St. Louis, MO). Peak areas were acquired with Agilent Chemstation software. NAA concentrations for MS and control brain tissue were determined in triplicate and statistical significance was determined with a Student's T test.

Respirometry

A Seahorse Bioscience XF 24 Extracellular Flux Analyzer (Seahorse Bioscience, Billerica, MA) was used to conduct real-time measurements of oxygen consumption and extracellular acidification (a measure of glycolysis) in SH-SY5Y cells according to the manufacturer's protocol. The oxygen consumption rate (OCR) in pmol O_2/min for respiration or the rate of extracellular acidification (ECAR) in mpH/min was measured simultaneously in SH-SY5Y cells before and after the addition of antimycin A. The optimal seeding density of SH-SY5Y cells, based on a measurable O_2 consumption and extracellular acidification rates was established, and both ECAR and OCR show a proportional response with cell number (data not shown). A seeding density of 150,000 cells per well was used for the experiment. OCR and ECAR measurements were made by a solid-state fluorescent oxygen and pH biosensor coupled to a fiber-optic waveguide. On the day of flux analysis, SH-SY5Y cells were checked under light microscope for an even confluent layer. The cells were rinsed twice, resuspended in 625 μl XF assay buffer with 2 mM sodium pyruvate and 4.5 g/L glucose (pH 7.4), and equilibrated for 50 min at 37°C in a non-CO_2 incubator. After cartridge calibration, the plate seeded with SH-SY5Y cells was loaded. After seven baseline measurements of OCR and ECAR, the mitochondrial complex III inhibitor antimycin A (1 μM) was injected into each well. OCR and ECAR values were calculated from four replicates by Seahorse wave software.

Assays for Measuring L-Aspartate and Acetyl-CoA Concentrations

Both L-aspartate and acetyl-CoA concentrations were measured by enzyme coupled colorimetric or fluorometric assays based on conversion of NAD^+ to NADH. For the aspartate assay, SH-SY5Y cells were seeded in 6 well plates overnight and treated with 2.5 μM antimycin A for 1 h and 4 h. L-Aspartate concentrations were measured using an aspartate assay kit (Sigma, Saint Louis MO). Briefly, cells were washed with ice-cold PBS twice and homogenized in 100 μl of aspartate assay buffer. The samples were centrifuged at 13,000g for 10 min to remove

cell debris, and the supernatant was collected. Samples were tested to ensure the readings were within the linear range of the standard curve. Absorbance at 570 nm was measured using a DTX 800 multimode detector (Beckman, Pasadena, CA). For the acetyl-CoA assay SH-SY5Y cells were seeded in 100 mm culture dishes overnight, and treated with 2.5 μM antimycin A for 1 and 4 h. Acetyl-CoA levels were measured using the picoprobe acetyl CoA assay kit (Biovision, Milpitas CA). Briefly, cells were washed twice with ice-cold PBS and incubated in 500 μl ice-cold cell lysis buffer with 200 mM Tris pH 7.5, 150 mM NaCl, 1 mM EDTA, 1 mM EGTA, 1 % Triton X-100, and Halt proteinase inhibitor cocktail (Fisher, Rockford IL) for 5 min. Cells were scraped off the plates and centrifuged at 13,000 g for 10 min. Background generated by free CoASH and succinate-CoA were corrected with 10 μl CoASH quencher in each well for 5 min at room temperature. Fluorescence intensity (λex = 535/λem = 589 nm) was measured using a DTX 800 multimode detector (Beckman, Pasadena, CA).

Aspartate and acetyl-CoA concentrations were normalized with protein concentration in each sample measured using the Bradford protein assay. The experiments were repeated twice with four replicates in each experiment. A Student's T test was performed to determine statistical significance between aspartate and acetyl-CoA concentrations measured in control and antimycin A treated SH-SY5Y cells.

Assay for Measuring Acetate Concentration

Acetate concentration was quantitated from normal appearing white matter (NAWM) tissue adjacent to the gray matter analyzed for NAA levels. For determination of acetate, 50–100 mg white matter tissue was polytron-homogenized in ddH_2O, then mixed with absolute ethanol 1:1 (vol:vol) and centrifuged at 10,000 g for 15 min. The supernatants were lyophilized and the dried residues were taken up in ddH_2O. The concentration of acetate was assayed via the method of Bartelt and Kattermann [27] using a Cary 300 spectrophotometer. Briefly, this assay detects the reduction of NAD^+ to NADH, by monitoring sample absorption at 365 nm from the following reactions.

Reactions

$$\text{Malate} + \text{NAD}^+ \overset{\text{MalateDehydrogenase}}{\longleftrightarrow} \text{Oxaloacetate} + \text{NADH} + \text{H}^+ \quad (1)$$

$$\text{Oxaloacetate} + \text{Acetyl}-\text{CoA} + \text{H}_2\text{O} \xrightarrow{\text{CitrateSynthase}} \text{Citrate} + \text{CoASH} \quad (2)$$

$$\text{Acetate} + \text{CoASH} + \text{ATP} \xrightarrow{\text{Acetyl}-\text{CoASynthetase}} \text{Acetyl}-\text{CoA} + \text{AMP} + \text{PPi} \quad (3)$$

Note that Reaction (1), which produces the spectrophotometrically-detected product, is reactant-favored, and is pulled to the right through the combined activities of the other two enzymes (if acetate is present).

Chemicals for these experiments were purchased from Sigma-Aldrich (St. Louis, MO). Buffer containing L-malate, ATP, CoASH and NAD^+ was combined with samples from MS and control brains, and a baseline 365 nm absorbance measurement was taken. A malate dehydrogenase / citrate synthase mixture was then added to the cuvettes, and a second 365 nm reading was collected three minutes later. Finally, acetyl-CoA synthetase was added to each cuvette, and incubated for 15 min, at which time a final 365 nm absorbance measurement was recorded. Acetate concentration was determined in duplicate for parietal cortex samples due to availability of tissue, and in triplicate for motor cortex samples and statistical significance was determined with a Student's T test. A Pearson's correlation test (Microsoft Excel) was performed to determine the significance of the correlation between decreased acetate and decreased NAA in MS and control samples.

Results and Discussion

In the present study we provide a link between mitochondrial activity and generation of NAA by mitochondria in SH-SY5Y neuroblastoma cells. NAA was quantitated in SH-SY5Y cells before and after treatment with the electron transport chain inhibitor antimycin A as shown in Fig. 2. Representative HPLC chromatograms for the NAA standard and for NAA measurements in SH-SY5Y cells are shown in Fig. 2a, b. A standard curve was also run with the NAA standard to be sure that measurements were taken in the linear range as shown in Fig. 2c. Quantitation for NAA measured with our HPLC method in control and antimycin

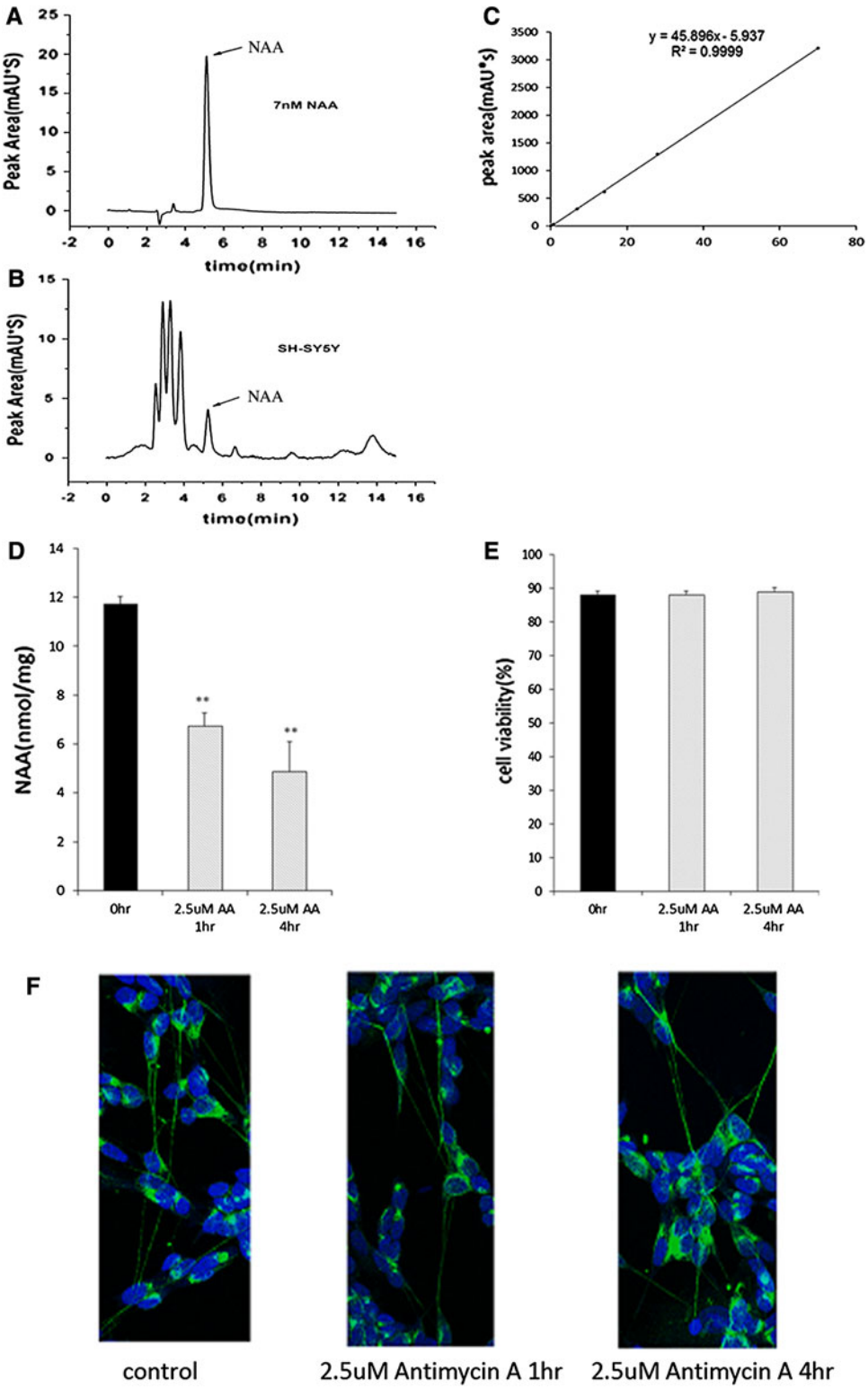

Fig. 2 Treatment with the electron transport chain inhibitor antimycin A reduced NAA levels in SH-SY5Y cells without inducing neuronal cell loss or degeneration of neurites. **a** Representative HPLC chromatogram showing NAA peak retention time of 5.10 min with an NAA standard solution. **b** Representative HPLC chromatogram showing the presence of the NAA peak in SH-SY5Y cells. **c**. HPLC peak areas in absorbance units (mAU*s) are a linear function of the amount of NAA (nmol) showing that NAA measurements were made within the linear range. **d**. Quantitation of NAA concentration by HPLC shows that 2.5 μM antimycin A (AA) reduced NAA levels in SH-SY5Y cells after 1 and 4 h treatments. Control SH-SY5Y cell NAA concentrations are shown by the *black bars* and AA treated cell NAA concentrations are represented by *gray bars*. *Error bars* denote SEM. $^{**}p<0.005$. **e** Cell viability assays performed on SH-SY5Y cells after treatment with 2.5 μm AA for 1 and 4 h show that cell numbers were not reduced. **f**. Cultures of SH-SY5Y cells were fixed and immunostained with an antibody to neurofilament (*green*) and Topro (*blue*) to stain nuclei. Numbers of neurites were counted and no significant neuritic loss was detected after AA treatment. Average number of neurites per cell was 2.83 ± 0.76 for control SH-SY5Y cells and 2.67 ± 0.64 for 4 h AA treated SH-SY5Y cells (Color figure online)

treated SH-SY5Y cells is shown in Fig. 2d. Our data show that treatment with antimycin A reduced NAA levels in SH-SY5Y cells by 40 % after 1 h and 50 % after 4 h of treatment. Cell viability after antimycin A treatment was determined by trypan blue staining and show that there was no decrease in viable cell numbers between control and

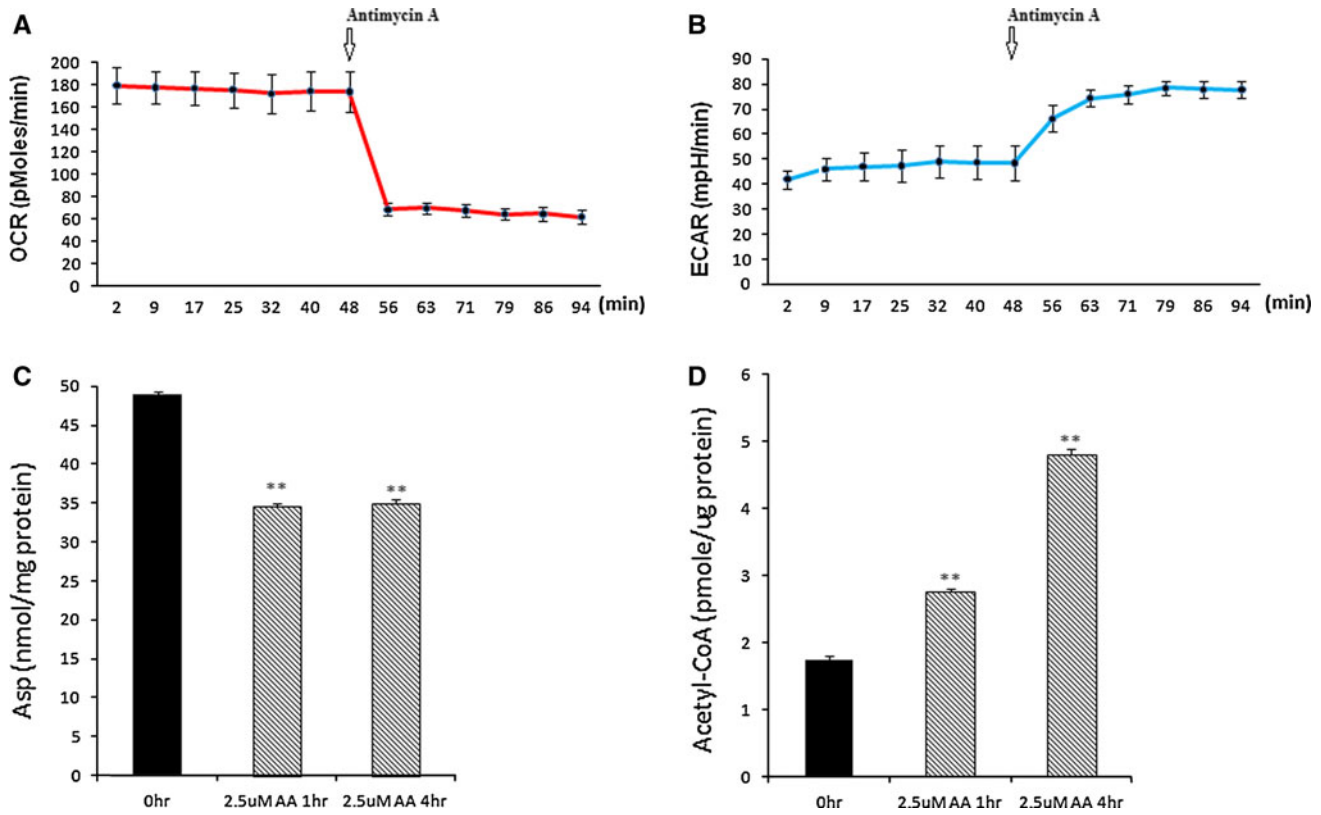

Fig. 3 The effect of antimycin A on respiration and levels of the NAA substrates, L-aspartate and acetyl-CoA, was determined in SH-SY5Y cells. OCR and ECAR were measured simultaneously in SH-SY5Y neuroblastoma cells before and after antimycin A treatment. **a** OCR rates (pmoles O_2/min) were measured in SH-SY5Y cells before and after antimycin A which was added at 48 min shown by the arrow. **b** The ECAR is a measure of glycolytic activity. ECAR (mpH/min) was measured simultaneously with OCR in SH-SY5Y cells before and after antimycin A treatment. **c** L-Aspartate concentrations decreased in SH-SY5Y cells after antimycin A (AA) treatment. Aspartate concentrations were measured in control SH-SY5Y cells (*black bar*) and in SH-SY5Y cells treated with antimycin A for either 1 or 4 h (*hatched bars*). **d** Acetyl-CoA concentrations increased after antimycin A treatment in SH-SY5Y cells. Acetyl-CoA concentrations were measured in control SH-SY5Y cells (*black bar*) and in antimycin A treated SH-SY5Y cells (*hatched bars*). *Error bars* denote SEM; $^{**}p < 0.01$

treated cells (Fig. 2e). Control and antimycin A treated SH-SY5Y cells were immunostained for neurofilament to assess the effects of antimycin A on neurite number and length. Images shown in Fig. 2f show that cell morphology and neurites remained intact in treated cells. We also performed respirometry on SH-SY5Y cells and showed that inhibition of complex III cytochrome c reductase with antimycin A decreased the OCR almost threefold from 180 to 60 pmol/min (Fig. 3a). Non-mitochondrial oxygen consumption was measured after rotenone treatment and found to be 31 pmol/min (data not shown) indicating that antimycin A was partially blocking electron transport. This decreased OCR was sustained for the duration of the experiment (45 min) and as expected, the rate of glycolysis increased twofold in the same cells as shown in Fig. 3b. An increase in the rate of glycolysis provides a mechanism to continue the synthesis of ATP and to compensate for the inhibition of electron transport and ATP production by mitochondria. Our cell culture data presented in Figs. 2 and 3 taken together shows that decreased NAA after treatment with antimycin A was not due to cell death or degeneration of neurites in the SH-SY5Y cells and suggests that decreased mitochondrial activity contributes to the decreased levels of NAA observed.

The schematic in Fig. 1 shows metabolic pathways relevant to NAA synthesis and catabolism and their relationship to energy metabolism pathways. Metabolites and pathways measured or inhibited in our study either in SH-SY5Y cells (NAA, acetyl-CoA, aspartate, Complex III, O2 consumption, glycolysis) or in postmortem brain tissue (NAA and acetate) are shown in bold in Fig. 1. To better understand the effect of electron transport chain inhibition on NAA synthesis, we also quantitated levels of L-aspartate and acetyl-CoA, the substrates for NAA synthesis, in SH-SY5Y cells after treatment with antimycin A for 1 and 4 h as shown in Fig. 3c, d. Antimycin A treatment decreased aspartate levels by over 26 % at both time points and increased acetyl-CoA by 1.5-fold at 1 h and threefold after

4 h. These results suggest that aspartate rather than acetyl-CoA is limiting for NAA synthesis under these conditions and suggests that aspartate levels may be an important point of regulation for NAA synthesis. Our data in Fig. 3 show that inhibition of complex III leads to decreased OCRs and increased rates of glycolysis in SH-SY5Y cells. Under these conditions we also found that acetyl-CoA accumulated, presumably as a result of increased production of acetyl-CoA by glycolysis and decreased acetyl-CoA utilization by the citric acid cycle due to decreased electron transport chain activity. Decreased aspartate concentrations after antimycin A treatment in SH-SY5Y cells may reflect an imbalance in the NADH/NAD^+ ratio which has been shown to occur in cultured cells as a result of increased glycolysis and decreased flow of electrons through the respiratory chain [28]. When the NADH/NAD+ ratio is high, aspartate would be less available for NAA synthesis because it would be converted to oxaloacetate and subsequently to malate by the aspartate–malate shuttle to regenerate cytoplasmic NAD^+ so that the generation of ATP by glycolysis could continue (Fig. 1). In fact previous studies have shown that in isolated rat brain mitochondria, the synthesis of NAA is decreased by electron transport chain inhibitors and is related to the production of ATP [29, 30]. These studies support our data which show that NAA levels provide a marker for neuronal metabolism and suggest that decreased NAA previously reported in the MS brain may reflect a metabolic defect in addition to neuronal and axonal loss. This metabolic contribution to reduced NAA in MS has been inferred by an in vivo imaging study which concluded that reduced NAA measured by MRS cannot be entirely attributed to axonal loss alone [31].

To test the significance of decreased NAA on the potential for remyelination in the MS brain, we next measured NAA levels in gray matter and acetate levels in adjacent white matter from eleven MS and seven control postmortem cortical tissue blocks. Table 1 shows the age, sex, PMI, disease duration, cause of death, and lesion status for the donor tissue analyzed in this study. To determine lesion status, we immunostained sections with an antibody to PLP that were adjacent to the tissue analyzed for NAA and acetate content. Representative PLP immunostaining of NAGM and gray matter subpial lesions are shown in Fig. 4a, b. We then quantitated NAA levels in parietal and motor cortex tissue blocks by HPLC. NAGM was analyzed from parietal cortex in six MS and three control tissue blocks. We also analyzed both NAGM and tissue containing gray matter lesions from motor cortex from five MS and four control tissue blocks. Representative chromatograms for NAA quantitation in gray matter from control and MS cortex are shown in Fig. 5a. Quantitation of HPLC results shows that NAA is decreased by an average of 25 and 32 % in MS parietal and motor cortex respectively

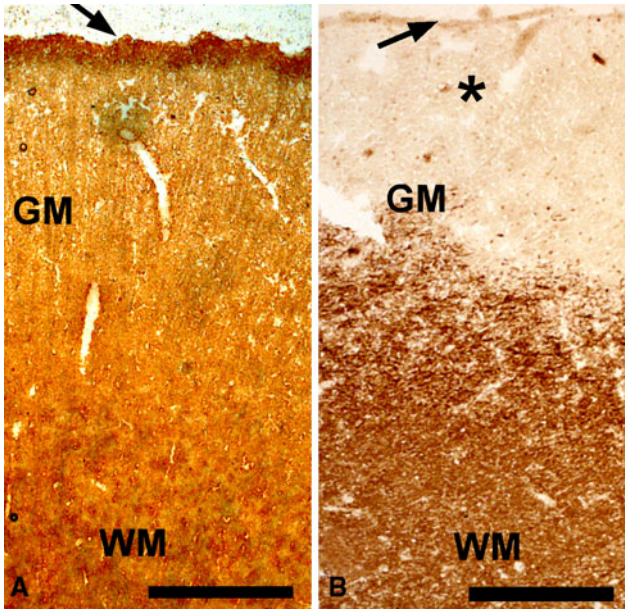

Fig. 4 Lesion status was determined by staining postmortem MS parietal and motor cortex tissue with a PLP antibody. Sections of motor cortex brain tissue (60 μm) were stained with a PLP antibody and the DAB reaction to localize lesions in the tissue slices. Staining patterns identified the cytoarchitecture of the motor cortex and PLP dense fibers could be seen streaming into the white matter (WM) perpendicular to the pial surface (*arrow*). Figures A and B display representative normal and lesioned tissue respectively acquired with 4× magnification. **a** In this micrograph normal appearing gray matter (GM) can be seen with a number of clearly visible cross-sectioned microvessels. **b** A subpial lesion (*asterisk*) is visible just below the pial surface (*arrow*) extending into the motor cortex GM. *Scale bar* represents 500 microns

compared to controls as shown in Fig. 5b. Our sample size isn't large enough to determine statistical significance of correlations between lesion status and NAA levels, however in our data set NAA levels do not appear to be correlated with lesion status in MS tissue. NAA was decreased in MS cortical gray matter compared to controls in both NAGM and in tissue containing gray matter lesions. Levels of NAA were decreased on average 32 % in NAGM compared to age and sex matched controls. In MS2, MS3, and MS5 which contained subpial gray matter lesions, NAA was decreased by 15, 26, and 25 %, respectively compared to controls (Fig. 6d). These results suggests that there is mitochondrial impairment leading to decreased NAA even in NAGM which is consistent with previous studies from our group and others which have reported mitochondrial defects in NAGM in MS [21–25].

To determine whether decreased NAA could be linked to decreased acetate concentrations in MS, we also measured levels of acetate in NAWM in the same tissue blocks in which we analyzed the NAA levels. We found that acetate concentrations were decreased in MS by 36 % in parietal cortex and 45 % in motor cortex compared to

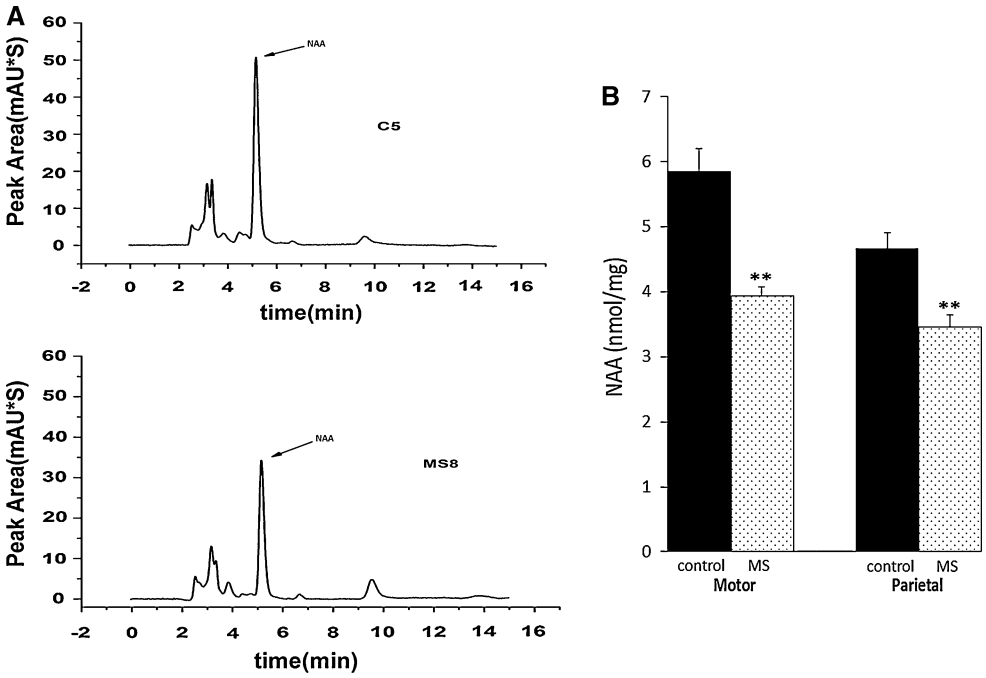

Fig. 5 NAA concentration is decreased in MS brain samples. **a** Representative HPLC chromatograms for control (*top*) and MS (*bottom*) cortical GM samples. *Arrow* denotes the NAA peak. **b** Quantitation of NAA concentration obtained by HPLC from 5 MS and 4 control motor cortex samples and 6 MS and 3 control parietal cortex samples shows significant decreases in mean NAA concentrations between control and MS groups. *Black bars* denote NAA concentrations for control samples and *dotted bars* represent NAA concentrations for MS samples. *Error bars* denote SEM. $^{**}p < 0.005$

controls (Fig. 6a). We then performed a Pearson's correlation analysis which showed that decreased acetate concentrations were correlated with decreased NAA concentrations in the postmortem brain samples ($r = 0.64$, $p < 0.01$) as shown in Fig. 6b. Comparing the data in matched pairs or groups we found that acetate was significantly decreased in nine out of the eleven MS samples compared to matched controls as shown in Fig. 6c. The concentration of acetate in white matter from postmortem MS brain tissue ranged from 0.035 to 0.123 mg/g and was higher on average in controls ranging from 0.098 to 0.139 mg/g as shown in Fig. 6c. These levels of acetate are consistent with brain acetate concentrations reported in another study which found 0.09 mg/g acetate in mouse brain [32]. Interestingly, in this same study, acetate concentrations were decreased to 0.02 mg/g in ASPA knockout mice which are unable to metabolize NAA to aspartate and acetate indicating that acetate concentrations in the brain are related to NAA catabolism. The two MS samples in which we did not detect decreased acetate concentrations were MS6 and MS10. We did not find decreased NAA or acetate in tissue from MS10. The tissue from MS6 was the only sample where we found decreased NAA that was not correlated with decreased acetate concentration. The autopsy report for MS6 noted no evidence of plaques even though the donor was diagnosed with MS indicating this may have been atypical MS.

Our data suggest that neuronal mitochondrial dysfunction may play a role in compromised myelination by oligodendrocytes in MS by limiting the availability of NAA derived acetate required for synthesis of myelin lipids. Acetate is the building block for fatty acid chain synthesis in lipid molecules and the role of acetate in myelination has been demonstrated in several studies. These studies have shown that NAA derived acetate is incorporated into myelin lipids [6, 7] and the lack of acetate due to a defective ASPA enzyme in Canavan's disease leads to dysmyelination [33]. Further, defective myelin lipid synthesis in ASPA knockout mice, a model of Canavan's disease, results from a deficiency of NAA-derived acetate [32]. We have shown that acetate is decreased in NAWM in MS, suggesting that there are alterations in white matter myelin which precede demyelination. Consistent with this finding several studies have reported that fatty acid composition and especially the very long-chain fatty acids, are altered in MS, even in NAWM compared with control brain white matter [34–37].

It has been previously shown that signals between neurons and glia are important for myelination. Neuronal activity in the form of action potentials leads to release of ATP by axons activating purinergic receptors on astrocytes. This results in the release of the cytokine leukemia inhibitory factor (LIF) by astrocytes. LIF then signals through LIF receptors on oligodendrocytes to increase expression of myelin proteins and the synthesis of myelin [38]. This intercellular signaling cascade between neurons and glia provides a mechanism for ensuring proper myelination of viable active neurons. The present study adds to the metabolic link between neurons and glia and suggests that NAA from axons may provide both energy necessary for myelination through increased acetate derived acetyl-CoA and may also promote myelination by increasing acetate for lipid synthesis. Our data suggest that in addition to regulation by neuronal electrical activity, myelination

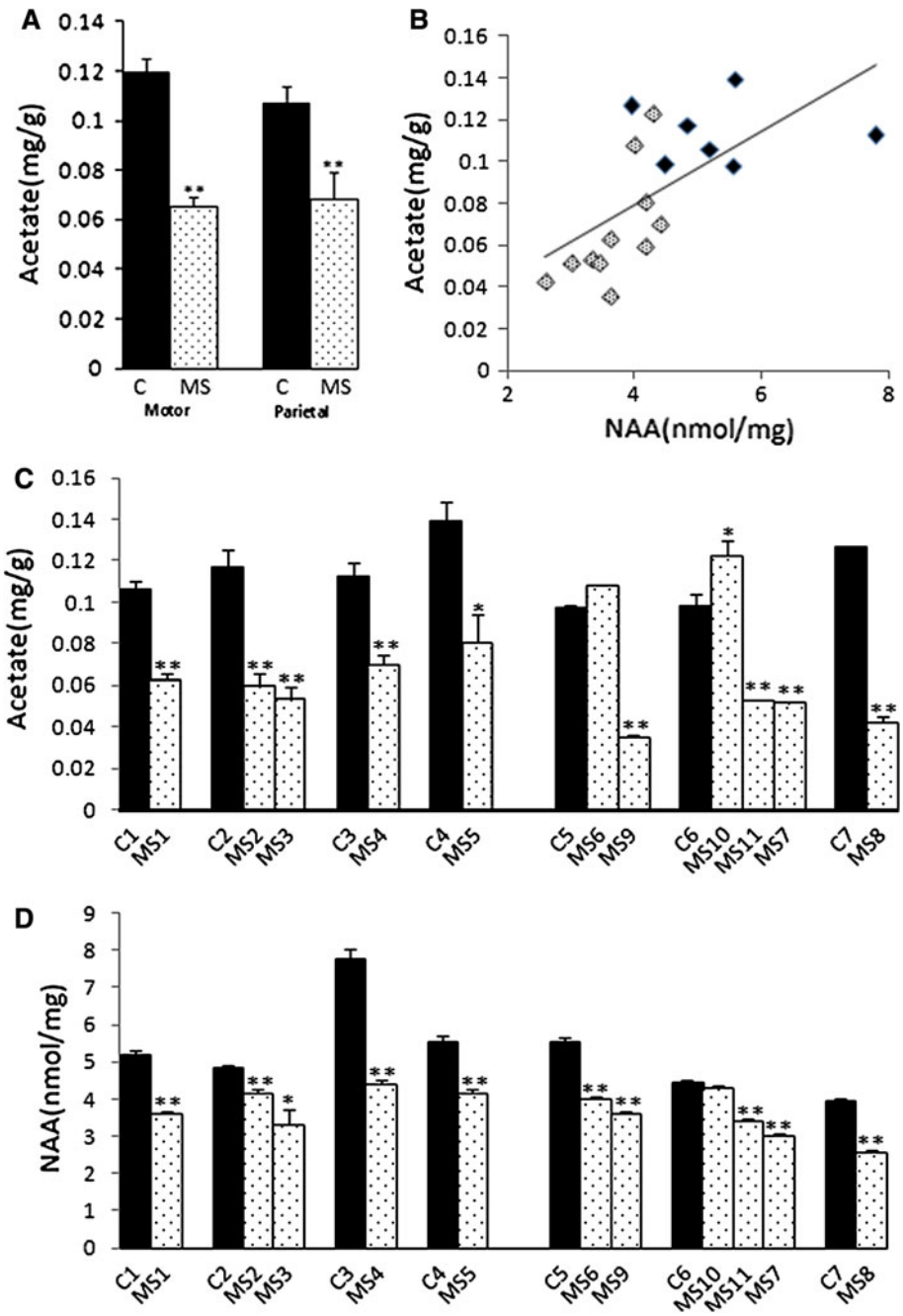

Fig. 6 Decreases in acetate concentration correlate with decreases in NAA concentration in MS brain samples. **a** Acetate concentrations are decreased in white matter in MS motor and parietal cortex compared to controls. Acetate was measured by a spectrophotometric method which measures the reduction of NAD^+ to NADH when free acetate is present as described in Materials and Methods. Acetate concentrations for control samples are represented by *black bars* and MS samples are represented by *dotted bars*. **b** A Pearson's correlation test was performed ($r = 0.64$; $p < 0.01$) and shows that acetate concentrations in MS white matter are correlated with NAA concentrations in adjacent GM. *Black filled squares* represent controls and *dotted squares* represent MS samples. **c** Acetate concentrations are shown for individual white matter samples. Comparisons are shown for MS samples (MS1–MS11) matched by sex, age, and PMI as closely as possible to a control (C1–C7). Quantitation shows that acetate is significantly decreased in 9 out of 11 MS samples compared to controls. **d** NAA concentrations are also shown for individual samples. NAA was measured in corresponding adjacent GM from the same control and MS pairs or groups shown in (**c**) Concentrations for controls (C1–C7) are represented by *black bars* and MS samples (MS1–MS11) are represented by *dotted bars*. *Error bars* denote SEM. $*p < 0.05$, $**p < 0.005$

may also be regulated by neuronal mitochondrial activity through synthesis of NAA to ensure myelination of healthy viable axons.

These results, along with our previous findings, suggest that neuronal mitochondrial dysfunction in MS cortex may be central to MS pathology and may contribute to impaired myelination and axonal damage through a loss of NAA. The initiating insult leading to mitochondrial defects in MS is not clear. Whether the initiating insult leading to mitochondrial damage is inflammatory in nature, or pathogen or toxin mediated is still under debate. Cortical lesions were found to be associated with meningeal inflammation in early stage disease in a study which analyzed biopsy material [39], but other studies analyzing postmortem tissue have not found evidence of inflammation or an association with meningeal inflammation in gray matter cortical lesions [17, 40]. In any case, accumulation of damage to mitochondria has been implicated as a pathological mechanism in MS [41]. Our results suggest that one mechanism by which mitochondrial dysfunction can lead to pathology in MS is through decreased synthesis of NAA. The resulting decrease in NAA in cortical neurons could

then decrease acetate and acetyl-CoA availability for energy metabolism and lipid synthesis in adjacent white matter oligodendrocytes. The consequence of these events could impair maintenance and stability of the myelin sheath and lead to demyelination in deeper white matter structures. Our study underscores the need for further research to understand the underlying mechanisms leading to mitochondrial damage in MS and the relationship between neuronal mitochondrial dysfunction and progression of MS pathology.

Acknowledgments We would like to thank the Rocky Mountain MS Center Tissue Bank for supplying postmortem tissue for this study. We would also like to thank the donors and their families. This study was supported in part by a Grant from the National MS Society. This investigation was funded in part by NIH Grant R21NS058921 (JM), NIH Grant R21NS075645 (JM and EF), and Funding from the College of Arts and Sciences at Kent State University.

References

1. Noseworthy JH, Lucchinetti C, Rodriguez M, Weinshenker BG (2000) Multiple sclerosis. N Engl J Med 343(13):938–952
2. England JD, Gamboni F, Levinson SR, Finger TE (1990) Changed distribution of sodium channels along demyelinated axons. Proc Natl Acad Sci U S A 87(17):6777–6780
3. Vukusic S, Confavreux C (2003) Prognostic factors for progression of disability in the secondary progressive phase of multiple sclerosis. J Neurol Sci 206(2):135–137
4. Moffett JR, Arun P, Ariyannur PS, Garbern JY, Jacobowitz DM, Namboodiri AM (2011) Extensive aspartoacylase expression in the rat central nervous system. Glia 59(10):1414–1434
5. Mehta V, Namboodiri MA (1995) *N*-acetyl aspartate as an acetyl source in the nervous system. Brain Res Mol Brain Res 31(1–2):151–157
6. Chakraborty G, Mekala P, Yahya D, Wu G, Ledeen RW (2001) Intraneuronal *N*-acetyl aspartate supplies acetyl groups for myelin lipid synthesis: evidence for myelin-associated aspartoacylase. J Neurochem 78(4):736–745
7. Ledeen RW, Wang J, Wu G, Lu ZH, Chakraborty G, Meyenhofer M, Tyring SK, Matalon R (2006) Physiological role of *N*-acetyl aspartate: contribution to myelinogenesis. Adv Exp Med Biol 576:131–143 discussion 361–3
8. Bjartmar C, Kidd G, Mörk S, Rudick R, Trapp BD (2000) Neurological disability correlates with spinal cord axonal loss and reduced *N*-acetyl-aspartate in chronic multiple sclerosis patients. Ann Neurol 48:893–901
9. De Stefano N, Narayanan S, Francis GS, Arnaoutelis R, Tartaglia MC, Antel JP, Matthews PM, Arnold DL (2001) Evidence of axonal damage in the early stages of multiple sclerosis and its relevance to disability. Arch Neurol 58(1):65–70
10. Gonen O, Catalaa I, Babb JS, Ge Y, Mannon LJ, Kolson DL, Grossman RI (2000) Total brain *N*-acetyl aspartate: a new measure of disease load in MS. Neurology 54(1):15–19
11. Inglese M, Ge Y, Filippi M, Falini A, Grossman RI, Gonen O (2004) Indirect evidence for early widespread gray matter involvement in relapsing-remitting multiple sclerosis. Neuroimage 21:1825–1829
12. Mathiesen HK, Jonsson A, Tscherning T, Hanson LG, Andresen J, Blinkenberg M, Paulson OB, Sorensen PS (2006) Correlation of global *N*-acetyl aspartate with cognitive impairment in multiple sclerosis. Arch Neurol 63(4):533–536
13. Ge Y, Gonen O, Inglese M, Babb JS, Markowitz CE, Grossman RI (2004) Neuronal cell injury precedes brain atrophy in multiple sclerosis. Neurology 62(4):624–627
14. Cader S, Johansen-Berg H, Wylezinska M, Palace J, Behrens TE, Smith S, Matthews PM (2007) Discordant white matter *N*-acetyl aspartate and diffusion MRI measures suggest that chronic metabolic dysfunction contributes to axonal pathology in multiple sclerosis. Neuroimage 36(1):19–27
15. Khan O, Shen Y, Caon C, Bao F, Ching W, Reznar M, Buccheister A, Hu J, Latif Z, Tselis A, Lisak R (2005) Axonal metabolic recovery and potential neuroprotective effect of glatiramer acetate in relapsing-remitting multiple sclerosis. Mult Scler 11(6):646–651
16. Ciccarelli O, Altmann DR, McLean MA, Wheeler-Kingshott CA, Wimpey K, Miller DH, Thompson AJ (2010) Spinal cord repair in MS: does mitochondrial metabolism play a role? Neurology 74(9):721–727
17. Bö L, Geurts JJ, Mörk SJ, van der Valk P (2006) Grey matter pathology in multiple sclerosis. Acta Neurol Scand Suppl 183:48–50
18. Fisher E, Lee JC, Nakamura K, Rudick RA (2008) Gray matter atrophy in multiple sclerosis: a longitudinal study. Ann Neurol 64(3):255–265
19. Kutzelnigg A, Faber-Rod JC, Bauer J, Lucchinetti CF, Sorensen PS, Laursen H, Stadelmann C, Brück W, Rauschka H, Schmidbauer M, Lassmann H (2007) Widespread demyelination in the cerebellar cortex in multiple sclerosis. Brain Pathol 17(1):38–44
20. Liepert J, Mingers D, Heesen C, Bäumer T, Weiller C (2005) Motor cortex excitability and fatigue in multiple sclerosis: a transcranial magnetic stimulation study. Mult Scler 11(3):316–321
21. Dutta R, McDonough J, Yin X, Peterson J, Chang A, Torres T, Gudz T, Macklin WB, Lewis DA, Fox RJ, Rudick R, Mirnics K, Trapp BD (2006) Mitochondrial dysfunction as a cause of axonal degeneration in multiple sclerosis patients. Ann Neurol 59:478–489
22. Pandit A, Vadnal J, Houston S, Freeman E, McDonough J (2009) Impaired regulation of electron transport chain subunit genes by nuclear respiratory factor 2 in multiple sclerosis. J Neurol Sci 279:14–20
23. Broadwater L, Pandit A, Azzam S, Clements R, Vadnal J, Yong VW, Freeman EJ, Gregory RB, McDonough J (2011) Analysis of the mitochondrial proteome in multiple sclerosis cortex. BBA Mol Bas Dis 1812:630–641
24. Campbell GR, Ziabreva I, Reeve AK, Krishnan KJ, Reynolds R, Howell O, Lassmann H, Turnbull DM, Mahad DJ (2011) Mitochondrial DNA deletions and neurodegeneration in multiple sclerosis. Ann Neurol 69(3):481–492
25. Witte ME, Nijland PG, Drexhage JA, Gerritsen W, Geerts D, van Het Hof B, Reijerkerk A, de Vries HE, van der Valk P, van Horssen J (2013) Reduced expression of PGC-1α partly underlies mitochondrial changes and correlates with neuronal loss in multiple sclerosis cortex. Acta Neuropathol 125(2):231–243
26. Rhein V, Baysang G, Rao S, Meier F, Bonert A, Müller-Spahn F, Eckert A (2009) Amyloid-beta leads to impaired cellular respiration, energy production and mitochondrial electron chain complex activities in human neuroblastoma cells. Cell Mol Neurobiol 29(6–7):1063–1071
27. Bartelt U, Kattermann R (1985) Enzymatic determination of acetate in serum. J Clin Chem Clin Biochem 23(12):879–881
28. Noda M, Yamashita S, Takahashi N, Eto K, Shen LM, Izumi K, Daniel S, Tsubamoto Y, Nemoto T, Iino M, Kasai H, Sharp GW, Kadowaki T (2002) Switch to anaerobic glucose metabolism with

NADH accumulation in the beta-cell model of mitochondrial diabetes. J Biol Chem 277(44):41817–41826
29. Clark JB (1998) N-acetyl aspartate: a marker for neuronal loss or mitochondrial dysfunction. Dev Neurosci 20(4–5):271–276
30. Signoretti S, Marmarou A, Tavazzi B, Lazzarino G, Beaumont A, Vagnozzi R (2001) *N*-acetyl aspartate reduction as a measure of injury severity and mitochondrial dysfunction following diffuse traumatic brain injury. J Neurotrauma 18(10):977–991
31. Ciccarelli O, Toosy AT, De Stefano N, Wheeler-Kingshott CA, Miller DH, Thompson AJ (2010) Assessing neuronal metabolism in vivo by modeling imaging measures. J Neurosci 30(45):15030–15033
32. Madhavarao CN, Arun P, Moffett JR, Szucs S, Surendran S, Matalon R, Garbern J, Hristova D, Johnson A, Jiang W, Namboodiri MA (2005) Defective N-acetyl aspartate catabolism reduces brain acetate levels and myelin lipid synthesis in Canavan's disease. Proc Natl Acad Sci U S A 102(14):5221–5226
33. Kaul R, Gao GP, Balamurugan K, Matalon R (1993) Cloning of the human aspartoacylase cDNA and a common missense mutation in Canavan disease. Nat Genet 5(2):118–123
34. Cumings JN, Goodwin It (1968) Sphingolipids and phospholipids of myelin in multiple sclerosis. Lancet II:664–665
35. Gerstl B, Eng LF, Tavaststjerna MG, Smith JK, Kruse SL (1970) Lipids and proteins in multiple sclerosis white matter. J Neurochem 17:677–689
36. Clausen J, Hansen IB (1970) Myelin constituents of human central nervous system. Acta Neurol Scand 46:1–17
37. Husted CA, Matson GB, Adams DA, Goodin DS, Weiner MW (1994) In vivo detection of myelin phospholipids in multiple sclerosis with phosphorus magnetic resonance spectroscopic imaging. Ann Neurol 36(2):239–241
38. Ishibashi T, Dakin KA, Stevens B, Lee PR, Kozlov SV, Stewart CL, Fields RD (2006) Astrocytes promote myelination in response to electrical impulses. Neuron 49(6):823–832
39. Lucchinetti CF, Popescu BF, Bunyan RF, Moll NM, Roemer SF, Lassmann H, Brück W, Parisi JE, Scheithauer BW, Giannini C, Weigand SD, Mandrekar J, Ransohoff RM (2011) Inflammatory cortical demyelination in early multiple sclerosis. N Engl J Med 365:2188–2197
40. Kooi EJ, Geurts JJ, van Horssen J, Bø L, van der Valk P (2009) Meningeal inflammation is not associated with cortical demyelination in chronic multiple sclerosis. J Neuropathol Exp Neurol 68(9):1021–1028
41. Witte ME, Geurts JJ, de Vries HE, van der Valk P, van Horssen J (2010) Mitochondrial dysfunction: a potential link between neuroinflammation and neurodegeneration? Mitochondrion 10(5):411–418